J. Fluid Mech. (1989), *vol.* 201, *pp.* 543–565
Printed in Great Britain

Monopole emission of sound by asymmetric bubble oscillations. Part 2. An initial-value problem

By MICHAEL S. LONGUET-HIGGINS†
Center for Studies of Nonlinear Dynamics, La Jolla Institute, 7855 Fay Ave., La Jolla, CA 92037, USA

(Received 16 June 1988 and in revised form 30 September 1988)

In Part 1 it was shown that an asymmetric, normal-mode bubble oscillation will emit monopole radiation at second order. Here we show that a general initial distortion of the bubble, with no initial volume change, can be resolved into normal modes each of which radiates independently. The zero-order 'breathing mode' is stimulated also.

Because of the peculiar damping characteristics, and the possibility of a resonance between the distortion modes and the breathing mode, the pulse of sound produced by the initial distortion will appear to have approximately the frequency of the breathing mode.

The conclusions are borne out in some detail by a comparison with the experiments of Fitzpatrick & Strasberg (1957) on the underwater sound generated by bubbles breaking away from a nozzle. A similar mechanism may contribute significantly to the generation of sound at the sea surface.

1. Introduction

In a previous paper (Longuet-Higgins 1989; referred to hereafter as Paper I) we showed that contrary to expectation a bubble oscillating in a normal distortion mode will, at second order, emit sound as in an ordinary monopole source of radiation. The effect is closely analogous to the generation of low-frequency sound by standing waves on the surface of deep water, or by oppositely travelling wave systems (see Longuet-Higgins 1950, 1953; Kibblewhite 1987). In the case of bubbles, the order of magnitude of the effect is such that it becomes an interesting mechanism for the generation of underwater sound in the ocean, especially at low wind speeds.

The present paper continues the investigation in Paper I by considering the following initial-value problem: Suppose a bubble, during the process of formation, has a distorted shape, which for simplicity we asume to be axisymmetric, as in figure 1. Suppose also that its volume is no different from that of the equilibrium sphere containing the same amount of air. What is the sound signal emitted from the bubble at subsequent times?

At first order in the distortion amplitude the initial distortion can be resolved into the sum of spherical harmonics, and we show in §2 that each harmonic, at second order, radiates sound independently of the others. Then in §3 we solve the initial-value problem in the case of a particular form of initial distortion (see figure 1). The

† Permanent address: Department of Applied Mathematics and Theoretical Physics, Silver Street, Cambridge CB3 9EW, UK.

amplitude of the sound from a given harmonic is shown to be particularly enhanced when its frequency (which is double that of the linear oscillation) is almost in resonance with the zero-order 'breathing mode'. For simplicity, damping is at first neglected.

The various kinds of damping are examined in §§4 and 5. Lamb's formula for the viscous damping is shown to provide, at best, an order-of-magnitude estimate. However, thermal and radiation damping, which affect the second-order monopole emissions, may dominate the sound pulse initially. Since the combined damping is at a minimum close to the resonant frequency of the breathing mode, the form of the pulse has predominantly this frequency.

Some detailed calculations are presented in §6, and in §7 we make a comparison with the experiments of Fitzpatrick & Strasberg (1957). A discussion on the significance of the mechanism for sound production in the ocean follows in §8.

Throughout this paper we use the notation already defined in Paper I. Reference to equations in that paper are prefixed by the symbol I.

2. The general asymmetric case

A general asymmetric disturbance will be given, to first order, by expressions of the form

$$\left.\begin{aligned} \eta_1 &= \sum_{n,l} a_{n,l}(t)\, S_n(\theta,\phi), \\ \Phi_1 &= \sum_{n,l} b_{n,l}(t) \left(\frac{a}{r}\right)^{n+1} S_n(\theta,\phi), \end{aligned}\right\} \tag{2.1}$$

where the sum is over all spherical harmonics of degree n and order l. We shall here discuss in particular the asymmetric case when $l = 0$ and so $S_n = P_n(\cos\theta)$, though some of our results may be generalized, as in (I) §9. To fix the ideas let us take

$$\left.\begin{aligned} \eta_1 &= \sum_n a_n S_n(\theta), \\ \Phi_1 &= \sum_n b_n \left(\frac{a}{r}\right)^{n+1} S_n(\theta), \end{aligned}\right\} \tag{2.2}$$

where a_n and b_n are given by I(6.6) and the frequency σ_n is given by I(6.7). We suppose there is no zero-order modal component, at first order. Then at second order, corresponding to I(6.11), for example, we shall have an equation of the form

$$\eta_{2t} - \Phi_{2r} = \frac{1}{a^2} \sum_{n,m} a_n b_n [(m+1)(m+2) S_n S_m - S_{n\theta} S_{m\theta}], \tag{2.3}$$

the double sum being taken over all positive values of both m and n. The general products $S_n S_m$, $S_{n\theta} S_{m\theta}$ etc., may be expressed in terms of spherical harmonics of degree not greater than $(n+m)$. However, as in §6 of Paper I, we are interested only in the monopole term, which can be obtained by averaging each side of the boundary condition (2.3), for example, over the unit sphere. Then we may make use of

LEMMA C

$$\overline{S_n S_m} = \left\{\begin{aligned} &\frac{1}{2n+1}, && m = n \\ &0, && m \neq n \end{aligned}\right\} \tag{2.4}$$

and

LEMMA D

$$\overline{\nabla_S S_n \cdot \nabla_S S_m} = \begin{cases} \dfrac{n(n+1)}{2n+1}, & m = n \\ 0, & m \neq n \end{cases} \tag{2.5}$$

to eliminate all products in which $m \neq n$; the right-hand side of the averaged equation (2.3), for example, reduces to a simple sum:

$$\bar{\eta}_{2t} - \bar{\Phi}_{2r} = \sum_n \frac{a_n b_n}{a^2}[(n+1)(n+2)\overline{S_n^2} - \overline{S_{n\theta}^2}], \tag{2.6}$$

with a similar sum for the other boundary condition. Hence the total contribution to the monopole radiation at second order is simply the sum of the contributions of the individual modes: i.e.

$$\bar{p}_2 = \sum_n \bar{p}_{2n} \tag{2.7}$$

where $\bar{p}_{2n}$ is given by I(7.1). There are no further interaction terms.

3. An initial-value problem

Let us consider the situation in which the fluid is initially at rest everywhere, but the bubble surface is distorted by a given amount. For example, let us assume that at time $t = 0$ the radial displacement η_1 is given by

$$\eta_1 = \epsilon a\left(\frac{1+\cos\theta}{2}\right)^s - C. \tag{3.1}$$

where s is a positive integer and C is a constant to be chosen so that

$$\bar{\eta}_1 = 0, \tag{3.2}$$

i.e. there is no initial change in the volume of the bubble.

For large values of s we have approximately

$$\eta = \epsilon a\, \mathrm{e}^{-s\theta^2/4} - C. \tag{3.3}$$

This is a Gaussian curve with width proportional to $s^{-\frac{1}{2}}$, very nearly; the height is reduced to half the maximum height when $\theta = \pm\theta_1$, where

$$\theta_1 = \left(\frac{\ln 16}{s}\right)^{\frac{1}{2}} = 1.63\, s^{-\frac{1}{2}}. \tag{3.4}$$

Since the expression (3.1) is a polynomial of degree s in $\mu = \cos\theta$, it may be expressed as a finite series of Legendre polynomials:

$$\eta_1 = \sum_{n=1}^{s} A_n P_n(\mu), \tag{3.5}$$

where, by the orthogonality relation (2.4),

$$A_n = (n+\tfrac{1}{2})\frac{\epsilon a}{2^s}\int_{-1}^{1}(1+\mu)^s P_n(\mu)\,\mathrm{d}\mu. \tag{3.6}$$

(*a*)

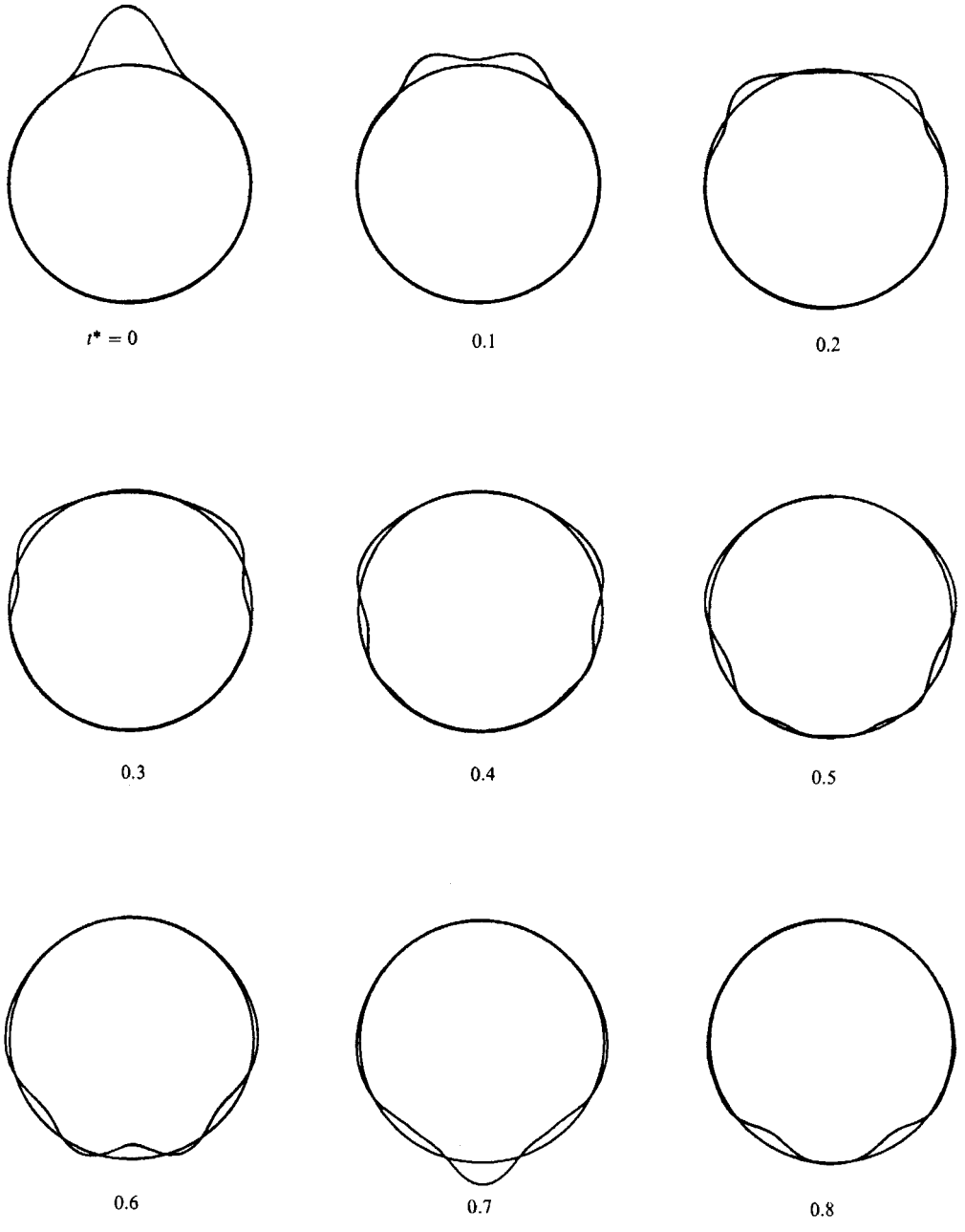

FIGURE 1 (*a*). For caption see page 548.

(*b*)

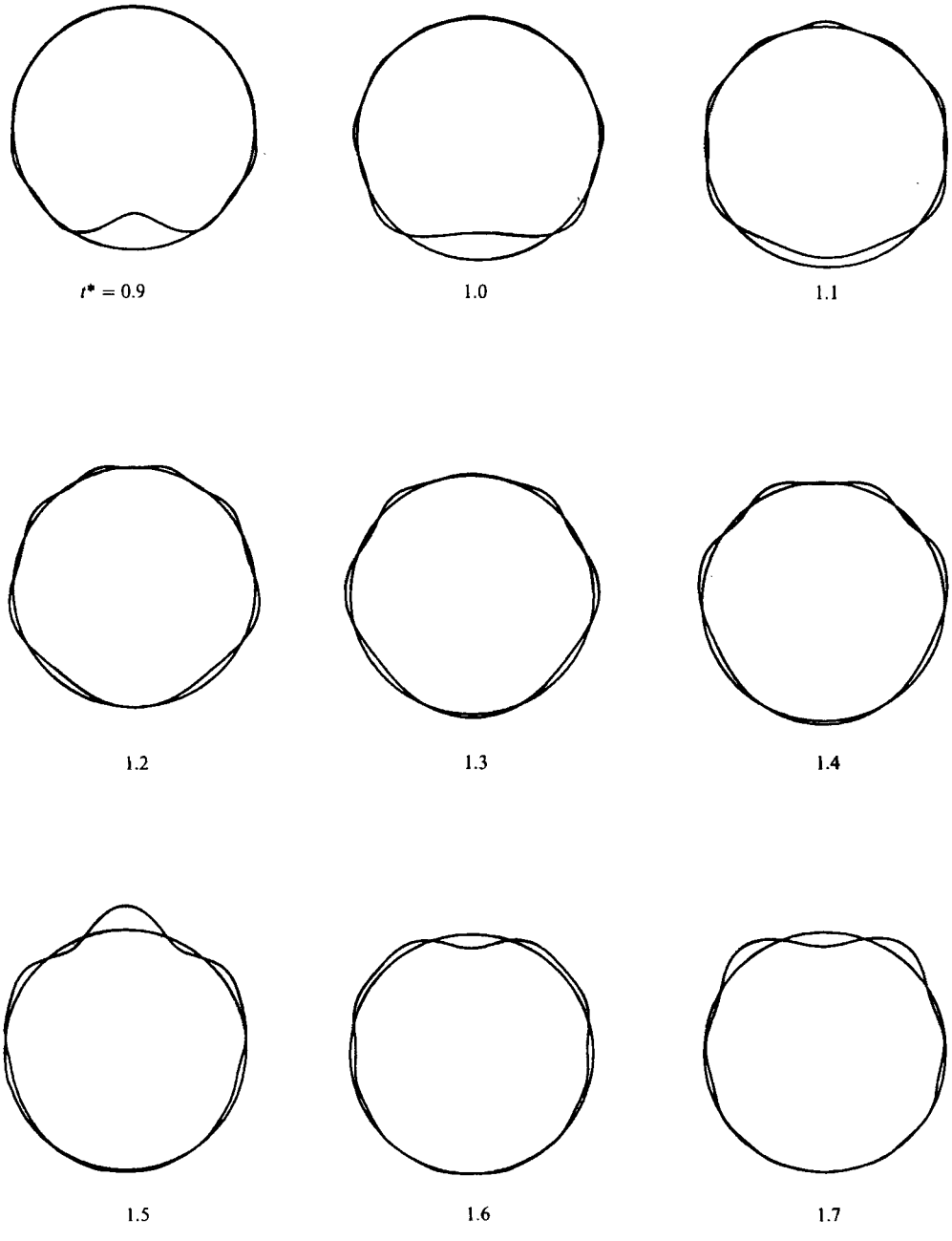

FIGURE 1 (*b*). For caption see next page.

(*c*)

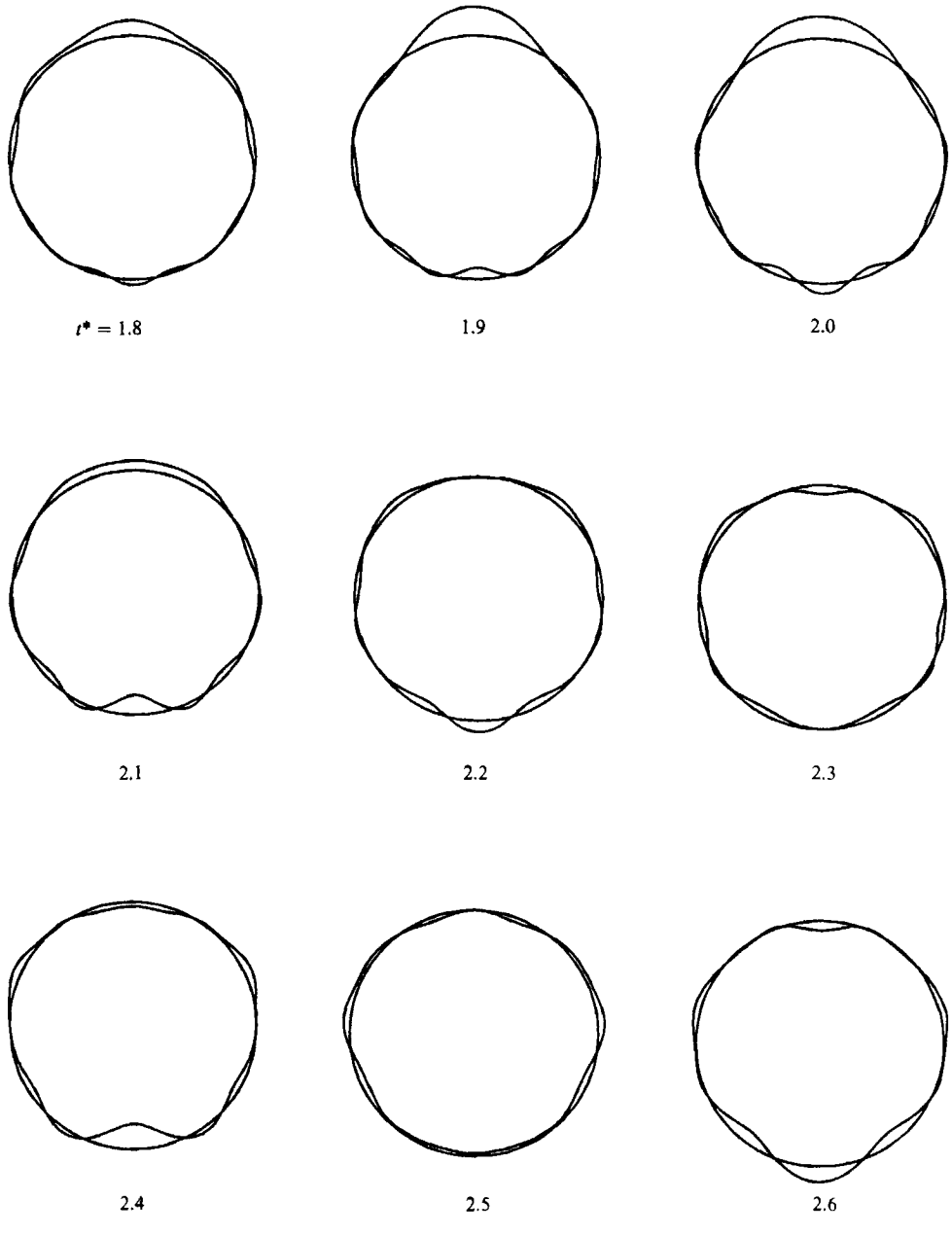

FIGURE 1 (*a–c*). Development of the surface profile given by equation (3.1) in the case $\epsilon = 0.5$.

By use of Rodriguez' formula

$$P_n(\mu) = \frac{1}{2^n n!}\frac{\mathrm{d}^n}{d\mu^n}(\mu^2-1)^n \tag{3.7}$$

and integration by parts, the integral in (3.6) is reduceable to a beta-function (see for example Erdelyi *et al.* 1953). Hence

$$A_n = \begin{cases} \epsilon a \dfrac{(2n+1)\,(s!)^2}{(s-n)!\,(s+n+1)!}, & n \leqslant s, \\ 0, & n > s. \end{cases} \tag{3.8}$$

Moreover

$$C = -A_0 = -\frac{\epsilon a}{s+1}. \tag{3.9}$$

By I §6, the first-order part of the solution is then given by

$$\left.\begin{aligned} \eta_1 &= \sum_n A_n P_n(\cos\theta)\cos\sigma_n t, \\ \Phi_1 &= \sum_n \frac{a\sigma_n}{n+1} A_n \left(\frac{a}{r}\right)^{n+1} P_n(\cos\theta)\sin\sigma_n t. \end{aligned}\right\} \tag{3.10}$$

As an example we show computations for the case when $\epsilon = 0.5$ and $s = 50$. By (3.4) this corresponds to an initial half-width $\theta_1 = 13.2°$. The coefficients A_n, $n = 1$ to 20, are given in table 1. The two largest coefficients, which are almost equal in magnitude, correspond to $n = 4$ and 5.

The development of the resulting disturbance can be seen in figure 1, where polar cross-sections of the bubble are shown at equal intervals of the dimensionless time

$$t^* = (T/a^3)^{\frac{1}{2}} t \tag{3.11}$$

up to $t^* = 3.0$. We see that the energy at first propagates away from the original disturbance at the pole $\theta = 0$, but subsequently converges toward the antipole $\theta = \pi$. The maximum disturbance at the antipole occurs when $t^* = 0.9$. Now since the mean wavelength of the nth harmonic is $2\pi a/n$, we may take the wavenumber roughly as $k = n/a$. Then the group velocity of the dominant waves may be calculated as

$$c_g = \frac{\Delta\sigma}{\Delta k} = \frac{\sigma_5 - \sigma_4}{5/a - 4/a} = 3.47\,(T/a)^{\frac{1}{2}} \tag{3.12}$$

in dimensional units. (This may be compared to the group velocity of a plane surface-tension wave which is $\frac{3}{2}(T/k)^{\frac{1}{2}}$. When $k = 4.5/a$ we have $c_g = 3.18(T/a)^{\frac{1}{2}}$). The time t^* for the energy to travel a distance πa is therefore

$$t^* = \frac{a\pi}{c_g}\left(\frac{T}{a^3}\right)^{\frac{1}{2}} = \frac{\pi}{3.47} = 0.91, \tag{3.13}$$

in agreement with figure 1.

A second convergence, this time at $\theta = 0$, occurs when $t^* = 1.9$ and again at $\theta = \pi$ when $t^* = 2.9$. By this time, however, the energy is quite dispersed. Note that we have so far neglected all forms of damping.

n	$A_n/\epsilon a$	n	$A_n/\epsilon a$
1	0.0566	11	0.0331
2	0.0872	12	0.0223
3	0.1085	13	0.0143
4	0.1192	14	0.0087
5	0.1196	15	0.0051
6	0.1116	16	0.0028
7	0.0977	17	0.0015
8	0.0807	18	0.0008
9	0.0631	19	0.0004
10	0.0469	20	0.0002

TABLE 1. Coefficients A_n for the initial-value problem of equation (3.1)

To find the second-order part of the motion we have to solve

$$\left.\begin{aligned} h_{2t}-\bar{\Phi}_{2r} &= 0, \\ \Phi_{2t}-a\omega^2 h_2 &= \sum_n (M\cos 2\sigma_n t+N) \end{aligned}\right\} \tag{3.14}$$

on $r = a$, where ω denotes the frequency of the free radial mode, see I(2.2), and M and N are given by I(6.24) and I(6.25), subject to the initial conditions that

$$h_{2t} = 0, \quad \Phi_2 = 0, \quad h_2 = 0 \tag{3.15}$$

when $t = 0$. The third condition states that there is no difference in volume between the initial volume and the volume of the equilibrium bubble.

Equations (3.14) are satisfied by assuming that

$$\left.\begin{aligned} h_2 &= \sum_n (X\cos 2\sigma_n t+Y-W\cos\omega t), \\ \bar{\Phi}_2 &= \frac{a}{r}\sum_n (Z\sin 2\sigma_n t-a\omega W\sin\omega t), \end{aligned}\right\} \tag{3.16}$$

where X, Y and Z are constants given by I(6.27) and where W is to be determined. The terms multiplying W represent a free radial oscillation which is excited at time $t = 0$.

The first two initial conditions in (3.15) are already satisfied. To satisfy the third, we must have

$$W = X+Y, \tag{3.17}$$

hence

$$W = \frac{M/a}{4\sigma_n^2-\omega^2}-\frac{N/a}{\omega^2}. \tag{3.18}$$

The pressure field at large distances is given by

$$p_2 = -\bar{\Phi}_{2t}. \tag{3.19}$$

On evaluating Z and W from the above equations we find after further reduction

$$p_2 = \frac{a}{r}\sum_n (P_n\cos 2\sigma_n t+Q_n\cos\omega t), \tag{3.20}$$

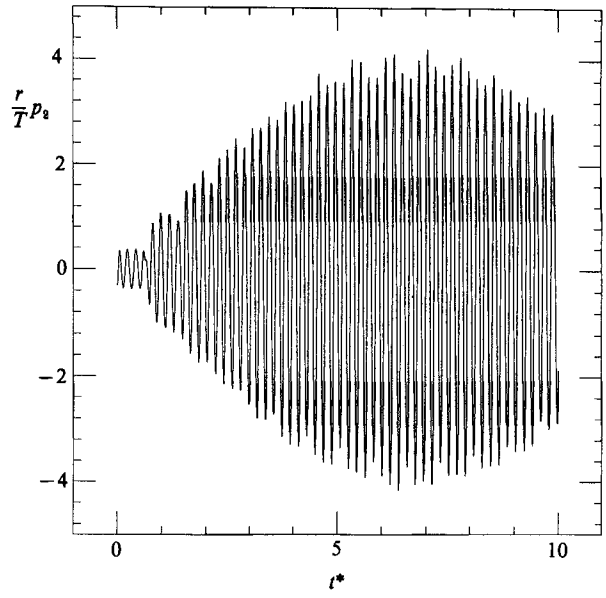

FIGURE 2. The monopole pressure field p_2 corresponding to figure 1, shown as a function of t^*, and when $a = 0.01948$ cm. No damping.

where
$$\left.\begin{aligned} P_n &= \frac{1}{\Omega^2-1}\frac{(n-1)(n+2)(4n-1)}{4(2n+1)}\frac{T}{a^3}A_n^2, \\ Q_n &= -\Omega^2 P_n + \frac{3(n-1)(n+2)}{4(2n+1)}\frac{T}{a^3}A_n^2 \end{aligned}\right\} \tag{3.21}$$

and we have written
$$\Omega^2 = \omega^2/4\sigma_n^2. \tag{3.22}$$

The dimensionless pressure field
$$p_2^* = rp_2/T, \tag{3.23}$$

i.e. the pressure at large distances, but without the factor $r^{-1}T$, was computed in the case corresponding to a bubble of radius $a = 0.01948$ cm, when
$$\omega = 33.000\ (T/a^3)^{\frac{1}{2}}. \tag{3.24}$$

In this case the radial mode is very nearly in resonance with the sixth harmonic, for which
$$2\sigma_6 = 33.466\ (T/a^3)^{\frac{1}{2}}. \tag{3.25}$$

The result is shown in figure 2, where p_2^* is plotted against the dimensionless time t^*. The most obvious feature is an almost sinusoidal variation of the wave envelope. This can be interpreted as a slow beat between the sixth mode of frequency $2\sigma_6$ and the radial mode of frequency ω.

Also in figure 2 one can see a smaller modulation of period $t^* = 0.88$ approximately. This appears to correspond to the time interval between successive convergence of energy at the poles, as shown earlier. Physically, because the second-order effects are proportional to the square of the local displacements, they produce a significant result on the radiated pressure only when the energy is sufficiently concentrated, that is at $t^* = 0$ and at subsequent polar convergences.

4. Viscous damping

We have so far assumed the flow near the bubble to be inviscid and irrotational. In reality, the presence of viscosity implies that at the surface of the bubble the two tangential components of the stress must be continuous, while the normal component, which includes a viscous term, has a given discontinuity due to surface tension. To accommodate these boundary conditions other types of solution of the viscous equations of motion are required.

In the first approximation, when the equations are linearized, and if the velocity vector is time-periodic, i.e.

$$\boldsymbol{u}' \propto \mathrm{e}^{\mathrm{i}\sigma t}, \tag{4.1}$$

then we find that

$$(\nabla^2 + h^2)\,\boldsymbol{u}' = 0, \tag{4.2}$$

where

$$h = (-\mathrm{i}\sigma/\nu)^{\frac{1}{2}} = (1-\mathrm{i})\,(\sigma/2\nu)^{\frac{1}{2}} \tag{4.3}$$

(see Lamb 1932, p. 352). Solutions to (4.2) exist in terms of functions

$$F_n(r,\theta,\phi) = (hr)^{-\frac{1}{2}} B_{n+\frac{1}{2}}(hr)\, S_n(\theta,\phi), \tag{4.4}$$

where $B_{n+\frac{1}{2}}$ denotes a Bessel function of order $(n+\frac{1}{2})$. Lamb (1881, 1932) solves the problem of an oscillating viscous sphere, when $\boldsymbol{u}$ is finite at the origin $r = 0$. For a bubble, on the other hand, we require solutions vanishing as $r \to 0$, and the appropriate Bessel functions are

$$K_{n+\frac{1}{2}}(z) = (-1)^n\,(\tfrac{1}{2}\pi)^{\frac{1}{2}} z^{n+\frac{1}{2}} \left(\frac{1}{z}\frac{\mathrm{d}}{\mathrm{d}z}\right)^n \frac{\mathrm{e}^{-z}}{z}, \tag{4.5}$$

with $z = hr$.

Just as for the liquid sphere, it may be shown that for an oscillating bubble the full boundary conditions can be satisfied by adding such terms to an irrotational flow. However, because of the exponential factor e^{-z} in (4.5) such terms contain factors

$$\mathrm{e}^{-h(r-a)} = \mathrm{e}^{-(1-\mathrm{i})\,(\sigma/2\nu)^{\frac{1}{2}}(r-a)} \tag{4.6}$$

which decay rapidly with distance away from the boundary, and describe boundary layers whose thickness Δ is of order

$$\Delta \sim (2\nu/\sigma_n)^{\frac{1}{2}}, \tag{4.7}$$

where σ_n is the radian frequency. Such 'Stokes layers' are already familiar in the theory of water waves (see Lamb 1932, C.11).

The viscous dissipation in the fluid surrounding the bubble may be calculated as though the flow were irrotational, but only if the Stokes layers are relatively thin, i.e. if $\Delta \ll a$. By (4.7) and I(6.7) this implies at least

$$a \gg \left(\frac{2\nu}{\sigma_n}\right)^{\frac{1}{2}} = \left[\frac{4\nu a^3}{(n^2-1)\,(n+2)\,T}\right]^{\frac{1}{4}}. \tag{4.8}$$

Taking $\nu = 0.013$ cm^2/s and $T = 75$ dyne/cm we have

$$[(n^2-1)\,(n+2)\,a]^{\frac{1}{4}} \gg 0.055 \tag{4.9}$$

in c.g.s. units. When $a = 0.01$ cm and $n = 2$, the left-hand side equals 0.39 cm$^{\frac{1}{4}}$ so that the inequality is apparently satisfied.

So it appears that we may calculate the dissipation D in the spherical harmonic

$$\Phi_1 = b_n \left(\frac{a}{r}\right)^{n+1} S_n(\theta, \phi) \tag{4.10}$$

from the formula

$$D = \nu \iiint \nabla^2 (\nabla \Phi_1)^2 \, \mathrm{d}\tau = -\nu \iint \frac{\partial}{\partial r} (\nabla \Phi_1)^2 \, \mathrm{d}S. \tag{4.11}$$

Hence
$$D = 4\pi (n+1)(n+2) \nu b_n^2 / a. \tag{4.12}$$

The kinetic energy, on the other hand, is given by

$$\mathrm{KE} = \frac{1}{2} \iiint \left(\nabla \Phi_1\right)^2 \mathrm{d}\tau = -\frac{1}{4} \iint \frac{\partial}{\partial r} \Phi_1^2 \, \mathrm{d}S. \tag{4.13}$$

Hence
$$\mathrm{KE} = \pi \frac{n+1}{2n+1} a \dot{b}_n^2. \tag{4.14}$$

In both (4.10) and (4.12) the coefficient $b_n(t)^2$ should be averaged with respect to the time. Since the average kinetic energy is only half the total energy, and since both are proportional to the square of the amplitude, the damping factors for the wave amplitude is $\mathrm{e}^{-\gamma_n t}$, where

$$\gamma_n = \frac{D}{4\mathrm{KE}} = \frac{(n+2)(2n+1)\nu}{a^2}. \tag{4.15}$$

This is equivalent to the formula given by Lamb (1932, p. 641).

On closer examination, however, we notice that in (4.11) the dissipation function $\nabla^2(\nabla \Phi_1)^2$ is proportional to $r^{-(2n+6)}$ which falls away almost exponentially with $(r-a)$. The thickness of the dissipation layer, on this basis, is of order $a/(2n+6)$, so that a more appropriate condition for the neglect of the Stokes layers is

$$\delta \ll a/(2n+6). \tag{4.16}$$

This suggests that (4.9) should really be replaced by

$$a^{\frac{1}{4}} \gg 0.55 \frac{2n+6}{[(n^2-1)(n+2)]^{\frac{1}{4}}}. \tag{4.17}$$

When $n = 2$, this implies

$$a^{\frac{1}{4}} \gg 0.30, \tag{4.18}$$

which can be considered to be satisfied only when a exceeds 1 cm. For larger values of n the condition (4.17) is even more stringent.

Thus it appears that Lamb's formula (4.13) is, at best, an order of magnitude estimate. We accept it as such for the present purpose. On this basis the relative decay of the amplitude per cycle would be

$$\frac{2\pi\gamma_n}{\sigma_n} = 2\pi \frac{(n+2)^{\frac{1}{2}}(2n+1)}{(n^2-1)^{\frac{1}{2}}} \frac{\nu}{(aT)^{\frac{1}{2}}}. \tag{4.19}$$

With $a = 0.02$ cm and $n = 2$, for example, the right-hand side has the value 0.39.

5. Total damping

Apart from viscous damping, the main energy loss may be expected to come from radiation due to the monopole terms, and from thermal effects.

The average flux of energy outwards from a monopole with velocity potential

$$\Phi = B\frac{a}{r}\sin\lambda(t-r/c) \tag{5.1}$$

(where λ is the radian frequency and c the speed of sound) is easily shown to be

$$F = 2\pi\lambda^2 a^2 B^2/c. \tag{5.2}$$

From (4.14) the total energy is

$$E = 2\pi a B^2. \tag{5.3}$$

Hence the damping factor $e^{-\gamma_R t}$ due to radiation alone would be given by

$$\gamma_R = F/2E = \lambda^2 a/2c. \tag{5.4}$$

We may compare this with Lamb's viscous damping factor (4.15). Setting $n = 0$, this gives

$$\gamma_V = 2\nu/a^2. \tag{5.5}$$

Thus

$$\gamma_R/\gamma_V = \lambda^2 a^2/4\nu c. \tag{5.6}$$

When, for instance $\lambda = 2\sigma_n$ this becomes

$$\gamma_R/\gamma_V = (n^2-1)(n+2)\,T/\nu c \tag{5.7}$$

which is independent of the bubble radius. However, since $T/\nu c = 0.041$, we see that for moderate values of n the two sources of damping are of comparable magnitude.

Thermal damping, along with viscous and radiation damping, was reviewed by Devin (1959), particularly in the case of resonant radial oscillations. Eller (1970) and Prosperetti (1977) have calculated the damping in forced radial oscillations and both show that for bubbles of given radius, thermal damping dominates at frequencies below resonance, while radiation damping dominates at frequencies above resonance. At resonance itself, the two are comparable.

For thermal damping, Eller (1970) defines

$$d_{TH} = \frac{3(\gamma-1)\,[\xi(\sinh\xi+\sin\xi)-2(\cosh\xi-\cos\xi)]}{\xi^2(\cosh\xi-\cos\xi)+3(\gamma-1)\,\xi(\sinh\xi-\sin\xi)}, \tag{5.8}$$

where

$$\xi = a(2\lambda/D_0)^{\frac{1}{2}}. \tag{5.9}$$

Here λ denotes the angular frequency of the forcing and D_0 is a thermal diffusivity for the gas; for air, $D_0 = 0.2$ cm^2/s. Then

$$\gamma^* = \frac{\gamma}{1+d_{TH}^2}\left[1+\frac{3(\gamma-1)\,(\sinh\xi-\sin\xi)}{\xi(\cosh\xi-\cos\xi)}\right]. \tag{5.10}$$

This quantity varies from 1, for bubbles pulsating isothermally, to 1.4, for bubbles pulsating adiabatically. Eller (1970) also defines

$$\omega^* = 3\gamma^* p_0/a^2. \tag{5.11}$$

The thermal damping coefficient corresponding to γ_V and γ_R is then

$$\gamma_{TH} = \frac{\omega^{*2}}{2\lambda} d_{TH}. \tag{5.12}$$

The total damping d_{TOT} may be specified by a dimensionless coefficient

$$d_{TOT} = \frac{2\lambda}{\omega^{*2}} (\gamma_V + \gamma_R + \gamma_{TH}). \tag{5.13}$$

Now to take into account the effects of damping, note that in (3.16) the terms with frequency $2\sigma_n$ will be affected by the following:

(1) The viscous losses from the linear mode, which we assume given by (4.12).

(2) The viscous losses from the second-order monopole, which we assume given by (4.12) with $n = 0$.

(3) The thermal and radiation losses from the second-order monopole, given by (5.2) and (5.12), with $\lambda = 2\sigma_n$.

The first loss is proportional to A_n^2, the second and third are proportional to A_n^4.

On the other hand the coefficient of $\sin \omega t$ in (3.16) receives no further energy after time $t = 0$; it arises solely from the initial conditions. It has only the second and third kinds of damping, that is to say

(4) Viscous losses given by (4.10) with $n = 0$ and b_n replaced by B_n.

(5) Thermal and radiation losses given by (5.2) and (5.12), with $\lambda = \omega$.

Since both (4) and (5) are proportional to B_n^2, this term will decay exponentially in the familiar way.

6. Numerical calculations

In order to calculate the rates of decay of the various modes we note that the total energy E_n of the nth mode contains significant contributions from both the first-order and the second-order oscillations. Thus we shall have generally

$$E_n = E_n^{(1)} + E_n^{(2)}, \tag{6.1}$$

where from (4.12)

$$E_n^{(1)} = 2\pi \frac{(n-1)(n+2)}{2n+1} T A_n^2. \tag{6.2}$$

In the second-order monopole oscillation, the kinetic energy is given by $\pi a P_n^2 / 4\sigma_n^2$, where P_n is the coefficient in (3.21), or more accurately the coefficient of a/r in (6.18). Since at resonance the kinetic and potential energies are equal, we have in general

$$E_n^{(2)} = (1 + \omega^2/4\sigma_n^2)\, \pi a P_n^2 / 4\sigma_n^2, \tag{6.3}$$

P_n being proportional to A_n^2. So altogether we will have for the dissipation D_n and the energy E_n two relations of the form

$$\left.\begin{aligned} D_n &= \alpha_1 y + \alpha_2 y^2, \\ E_n &= \beta_1 y + \beta_2 y^2, \end{aligned}\right\} \tag{6.4}$$

where $y = A_n^2$. If we assume that α_1, β_1, α_2 and β_2 remain constant during the process of decay, then from

$$\frac{dE_n}{dt} = -D_n \tag{6.5}$$

we obtain
$$\frac{\mathrm{d}y}{\mathrm{d}t} = -\frac{\alpha_1 y + \alpha_2 y^2}{\beta_1 + 2\beta_2 y}. \tag{6.6}$$

This has the implicit solution
$$t = -\frac{\beta_1}{\alpha_1}\ln y - \left(\frac{2\beta_2}{\alpha_2} - \frac{\beta_1}{\alpha_1}\right)\ln\left(y + \frac{\alpha_1}{\alpha_2}\right), \tag{6.7}$$

which shows that $y \to 0$ exponentially as $t \to \infty$. In practice, however, it is easier to determine $y(t)$ by numerical integration from (6.6).

For the free oscillation with frequency ω^*, the total energy E_0 is given by
$$E_0 = E_0^{(2)} \propto Q_n^2, \tag{6.8}$$

where Q_n is the amplitude. Since
$$D_0 = D_0^{(2)} \propto Q_n^2 \tag{6.9}$$

it follows that
$$E_0 \propto \mathrm{e}^{-2\gamma_0 t} \tag{6.10}$$

where γ_0 is the ordinary damping coefficient for resonant radial bubble oscillations.

The damping of the motion introduces small phase differences which in general can be ignored. In one context, however, these are important, namely in the response of the breathing mode to frequencies near resonance. We note that in (3.14), since $\bar{\Phi}_2 \propto 1/r$, we have
$$\bar{\Phi}_{2r} = -\frac{1}{a}\bar{\Phi}_2 \tag{6.11}$$

and so on differentiating the first of equations (3.14) with respect to t and eliminating $\bar{\Phi}_{2t}$ we get, for every $n \geqslant 2$,
$$h_{2tt} + \omega^2 h_2 = \mathrm{Re}\,(-M/a)\,\mathrm{e}^{2\mathrm{i}\sigma_n t} - N/a. \tag{6.12}$$

To include damping in the response we must add a term $2\gamma_0 h_{2t}$ to the left-hand side and replace ω by the modified frequency ω^*; see (5.11). The solution of this equation satisfying the initial conditions
$$h_2 = 0, \quad h_{2t} = 0. \tag{6.13}$$

Then $t = 0$ is
$$h_2 = \frac{-M/a}{(\omega^{*2} - 4\sigma_n^2) + 4\mathrm{i}\gamma_0\sigma_n}\mathrm{e}^{2\mathrm{i}\sigma_n t} - \frac{N}{a\omega^{*2}} - W\,\mathrm{e}^{-\gamma_0 t}\cos(\omega^{*2} - \gamma_0^2)^{\frac{1}{2}}t - W'\,\mathrm{e}^{-\gamma_0 t}\sin(\omega^{*2} - \gamma_0^2)^{\frac{1}{2}}t, \tag{6.14}$$

and the real part of the right-hand side is understood. From (6.13) we find
$$W = \frac{-(\omega^{*2} - 4\sigma_n^2)M/a}{(\omega^{*2} - 4\sigma_n^2)^2 + (4\gamma_0\sigma_n)^2} - \frac{N/a}{\omega^{*2}} \tag{6.15}$$

and
$$W' = \frac{\gamma_0}{(\omega^{*2} - \gamma_0^2)^{\frac{1}{2}}}\left[\frac{-8\sigma_n^2 M/a}{(\omega^{*2} - 4\sigma_n^2)^2 + (4\gamma_0\sigma_n)^2} + W\right]. \tag{6.16}$$

The pressure p_2 for large r can then be calculated from
$$p_2 = -\bar{\Phi}_{2t} = -\frac{a}{r}(\bar{\Phi}_{2t})_{r=a} = \frac{a^2}{r}(\bar{\Phi}_{2rt})_{r=a} \tag{6.17}$$

or from (3.14)

$$p_2 = \frac{a^2}{r} h_{2tt}. \tag{6.18}$$

From the above formulae we find that the pressure p_2 at the initial instant $t = 0$ is given by

$$(p_2)_{t=0} = -\frac{T}{r} \sum_n \frac{(n-1)^2 (n+2)}{2n+1} \frac{A_n^2}{a^2} \tag{6.19}$$

which is independent of both γ_0 and ω^*. Moreover, for bubbles of a given initial shape, the ratios A_n/a are constant. Equation (6.19) then shows, remarkably, that the initial pressure p_2 at a fixed distance r from the bubble is independent of the bubble radius a.

A physical explanation of this result can be given as follows. The pressure due to surface tension at the bubble is proportional to the mean curvature of the surface. Hence, for a bubble of given shape, the surface pressure is inversely proportional to the bubble radius a; for small bubbles it becomes very large. In fact its behaviour precisely matches the monopole behaviour of the pressure field itself, which varies inversely as r, when $r \gg a$. At first sight it seems incredible that a tiny bubble, however small its radius, can produce a finite effect at a fixed distance. The paradox is resolved when we consider that as the natural frequency of the bubble increases, so also does the damping, so that the pulse of energy emitted becomes increasingly short. (There are of course physical limits on bubble size due, for instance, to the absorption of gas across its surface.)

In the example of §3, when A_n/a is given by (3.8) with $\epsilon = 0.5$, we find

$$(p_2)_{t=0} = -0.307\ T/r. \tag{6.20}$$

The solution (6.18) was evaluated numerically for different bubble radii a. Some typical results are shown in figure 3. In each part of the figure the dominant frequency is at around the corresponding 'resonant' frequency ω. This is for two separate reasons: First, there are always some modes carrying substantial amounts of energy such that $2\sigma_n$ is nearly in resonance with ω; see I figure 2 and table 1. Secondly, the damping happens to be a minimum not far from the resonant frequency; see Eller (1970) and Prosperetti (1977).

In figure 3(*a*), the radius a is the same as in figure 2, that is $a = 0.01948$ cm, but the emitted pulse is different in two main respects. The damping is much greater, so that the pressure amplitude is now reduced to one-half its initial value in only 3 cycles (0.5 ms). Also the resonant frequency ω^* has been slightly altered by the damping, so that the beat between it and the harmonic $n = 6$ is now much shorter.

In figure 3(*b*), the bubble radius is increased to 0.05 cm, the resonant frequency ω^* of the pulse is longer and the damping is less. The same trend is contained in figure 3(*c*) ($a = 0.1$ cm) and in figure 3(*d*) ($a = 0.23$ cm). In figure 3(*d*) the resonance is at around $n = 14$ and the amplitude is halved in 6 cycles (4 ms).

The rates of damping are very similar to these calculated elsewhere; the main difference arises from the viscous (linear) damping in the distortion modes, which contributes (nonlinearly) to the damping of the monopole terms. The method of excitation of the monopole modes, and of the breathing mode, is of course very different from that previously envisaged.

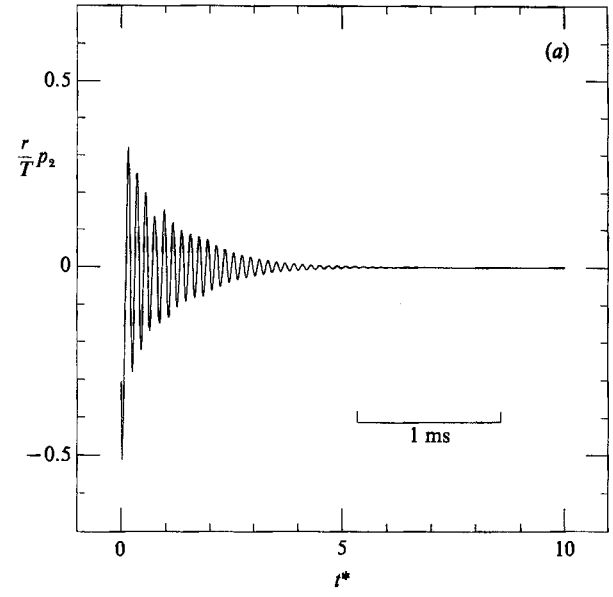

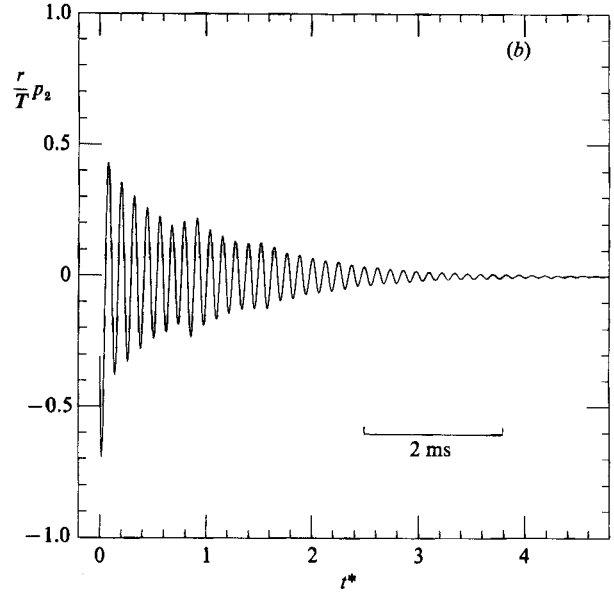

FIGURE 3(*a*, *b*). For caption see facing page.

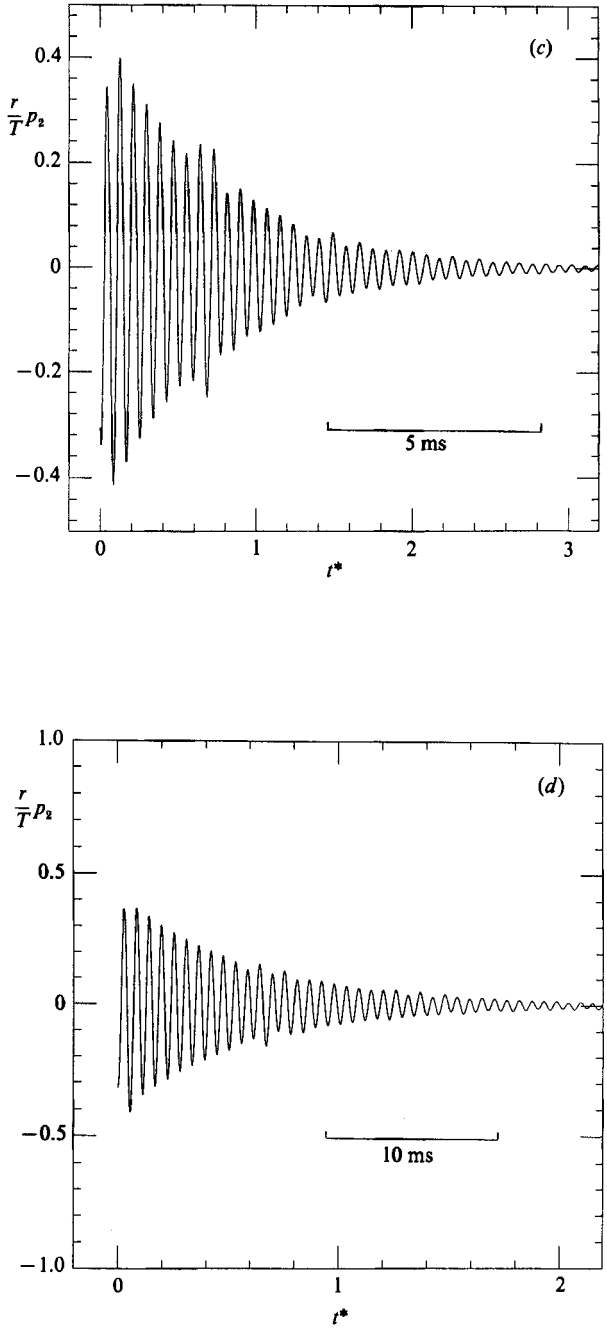

FIGURE 3. (*a*) As in figure 2, but with the addition of damping. (*b*) $a = 0.05$ cm. (*c*) $a = 0.10$ cm. (*d*) $a = 0.23$ cm.

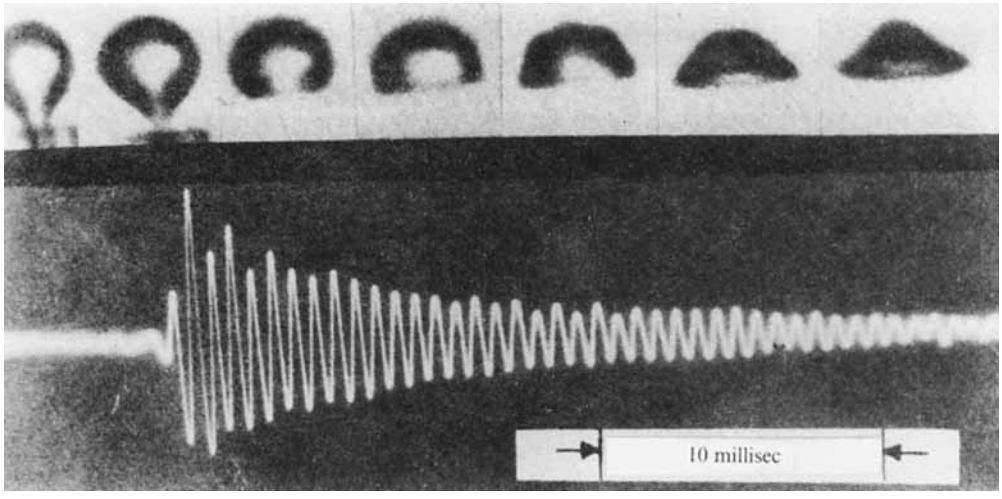

FIGURE 4. Oscillogram of the sound pulse from an air bubble formed at a nozzle, with synchronized photographs of the bubble (from Fitzpatrick & Strasberg 1957).

7. Comparison with observation

Figure 4, from Fitzpatrick & Strasberg (1957), shows the sound pulse produced by an air bubble as it breaks away from an underwater nozzle. The lengthscale is unspecified, but from the timescale and the frequency of the oscillation one can estimate the equilibrium radius a to be close to 0.23 cm, as in figure 3(d). The form of the pulse in figure 4 is evidently very similar to that in figure 3(d).

In the fifth frame of figure 4 one can see in the bubble silhouette some clear evidence of a harmonic of degree $n = 8$. From the discussion in §3, we would expect this to correspond to a group velocity

$$c_g = \tfrac{3}{2}(Tk)^{\frac{1}{2}}, \quad k = 8/a. \tag{7.1}$$

Hence the energy will be carried to the antipole in a time

$$t = \frac{\pi a}{c_g} = \frac{\pi}{3}\left(\frac{a^3}{2T}\right)^{\frac{1}{2}} = 9 \text{ ms} \tag{7.2}$$

and will appear again at the antipole when it is three times this amount, that is about 27 ms after the initial breakaway. This may account for the bulge in the upper side of the bubble which is seen in the seventh frame. There probably was a similar bulge between the fourth and fifth frames.

However, it was apparently not the harmonic $n = 8$ which was responsible for the sound pulse, but more probably the harmonic around $n = 14$, as indicated in §6 and figure 3(c).

One interesting feature of the observed pulse in figure 4 is the beat with period 2 cycles near the beginning of the pulse. This indicates the presence of a frequency component λ equal to one-half that of the resonant frequency, i.e.

$$\lambda = \tfrac{1}{2}\omega^* \approx \sigma_n. \tag{7.3}$$

We suggest that this could be the result of a third-order intersection. For, three frequencies $\lambda_1, \lambda_2, \lambda_3$ will generally interact to produce a frequency

$$\lambda_{123} = \lambda_1 \pm \lambda_2 \pm \lambda_3. \tag{7.4}$$

Thus, for example, if $\lambda_1 = \lambda_2 = \lambda_3 = \sigma_n$ one could have

$$\lambda_{123} = \sigma_n + \sigma_n - \sigma_n = \sigma_n. \tag{7.5}$$

We remark that the initial bubble shape seen in figure 4, frame 2, is actually somewhat sharper than in figure 5, at $t = 0$. Thus the harmonic $n = 14$ probably will be larger relative to the others. Generally we must envisage an initial bubble profile even more sharply pointed, possibly with an outward-pointing cusp. For such a form, the second-order theory given here is inadequate; to cope accurately with such a highly non-linear situation, fully nonlinear calculations will be required, using for example a boundary-integral technique.

8. Application to the ocean

There is now very strong evidence (see Farmer 1987; Farmer & Vagle 1988) that naturally occurring underwater sound in the ocean comes mainly from surface sources, particularly breaking waves and whitecaps, but also from rain and falling spray. At low wind speed it is possible that air pockets are entrained even in the absence of visible whitecaps (see Banner & Cato 1987; Longuet-Higgins 1988). A theory proposing that the emitted sound is due to the application of sudden additional pressures or velocities to a spherical bubble, just after it is formed, was given by Hollett & Heitmeyer (1987).

It is obvious, however, that in developing from a plane surface into a spherical bubble, the surface must pass through some intermediate and highly non-spherical forms. One possibility, for example, is that the familiar overturning of the surface in a breaking gravity wave, or in a steep capillary ripple, will at first trap a cylindrical pocket of air, which then will develop instabilities in a longitudinal direction. These will then grow so as to pinch off a closed 'sausage' of air. We note that the most rapidly growing instability of a hollow fluid cylinder has been shown by Chandrasekhar (1961) to have a length equal to about six times the diameter of the initial cylindrical cross-section.

Here we propose to make an estimate of the contribution from such distortions of the surface during the process of bubble formation.

Direct measurements of the rate of bubble formation in the ocean are are scarce, but from laboratory measurements Toba (1961) has estimated the mean rate of entrainment b of bubbles per unit time and per unit horizontal area of the sea surface, at given wind speeds. His results are reproduced in figure 1 of Paper I. At a wind speed of 11 m/s, for example, the most important bubble diameters are in the range 0.4 to 4 mm. Let us assume $2a = 2$ mm, so $a = 0.1$ cm. Toba's figure then indicates that

$$B = \frac{\mathrm{d}b}{\mathrm{d}(\ln a)} = 0.1 \text{ cm}^{-2}\text{ s}^{-1} \tag{8.1}$$

approximately, hence

$$b = \int_{2a=0.4}^{4} (0.1)\,\mathrm{d}(\ln a) = 0.3 \text{ cm}^{-2}\text{ s}^{-1}. \tag{8.2}$$

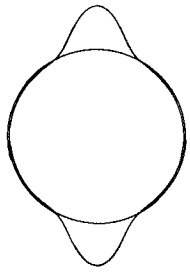

FIGURE 5. Assumed initial form of air pocket trapped near the sea surface.

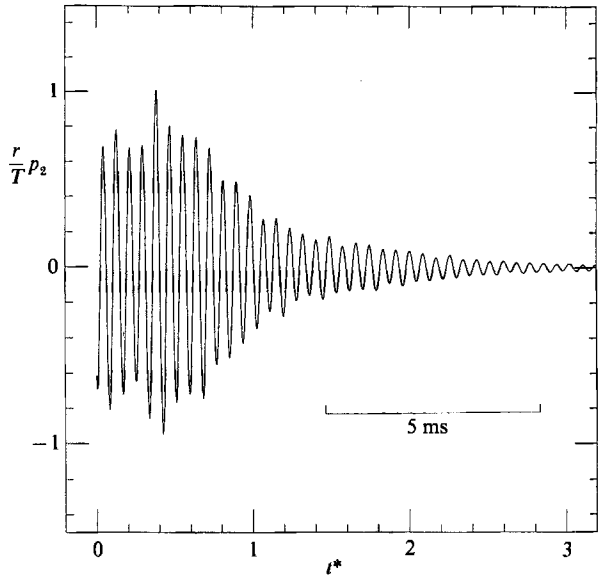

FIGURE 6. The pressure field corresponding to figure 5.

As a rough model one might consider an axisymmetric initial form similar to (3.1) but symmetrical in regard to the equator, that is to say with a second hump added at the antipole $\theta = \pi$ see figure 5. Thus we may assume that at time $t = 0$

$$\eta_1 = \epsilon a\left(\frac{1+\cos\theta}{2}\right)^s + \epsilon a\left(\frac{1-\cos\theta}{2}\right)^s - 2C. \tag{8.3}$$

The coefficient A'_n corresponding to this form will be related to the coefficient A_n of (3.8) by

$$A'_n = A_n[1+(-1)^n]. \tag{8.4}$$

The numerical computation of the pressure p_2 then proceeds as in §§3–6. In figure 6 $r/p_2/T$ is plotted against t^* in the case $a = 0.1$ cm, $\epsilon = 0.5$. The initial magnitude is of order

$$rp_2 = 0.75T = 3.0\ \epsilon^2 T\ \text{cm}^3/\text{s}^2 \tag{8.5}$$

in c.g.s. units. The duration of the pulse is of order

$$\tau = 4\ \text{ms}. \tag{8.6}$$

So for the mean-square pressure amplitude we have

$$P^2 = \langle (rp_2)^2 \rangle b\tau = 11\epsilon^4 \text{ (cm/s)}^4. \tag{8.7}$$

We assume that each bubble emits radiation independently of the others. However, the presence of the free surface implies the existence of an image for each bubble, tending to reduce the pressure amplitude by a factor of order $\omega z/c$, where ω is the radian frequency, z the distance of the bubble below the free surface and c the velocity of sound. Taking $z = 1$ cm and $\omega = 2 \times 10^4$ s^{-1}, at this bubble radius, we find

$$\frac{z\omega}{c} = 0.14 \tag{8.8}$$

approximately. For the total vertical flux of energy from all the source-image pairs we have

$$F_z = \pi \left(\frac{\omega z}{c}\right)^2 \frac{P^2}{c} \tag{8.9}$$

where P is given by (8.7). Hence altogether we obtain†

$$F_z = 5.0 \times 10^{-5}\, \epsilon^4 \text{ erg/cm}^2\text{/s}. \tag{8.10}$$

Now the above argument indicates that for the distortions that we are likely to encounter an approximate value of ϵ would be of order 6. For such large values of ϵ the perturbation analysis given earlier is hardly valid. Nevertheless, since the emission of the sound involves a high harmonic ($n = 11$) which may oscillate many times before the collapse of the bubble as a whole, the formula (8.10) may be expected to give still an order of magnitude for the sound intensity. In fact, if conservatively we substitute $\epsilon = 1$ into (8.10) we obtain

$$F_z = 5 \times 10^{-5} \text{ erg/cm}^2\text{/s}. \tag{8.11}$$

A typical underwater sound pressure at a wind speed of 11 m/s and at a depth 24 m below the surface, integrated over the frequency range 0.3 to 20 kHz, is 0.23 Pa, r.m.s. (D. M. Farmer, personal communication). This implies a flux density, not necessarily vertical, equal to 3.5×10^{-5} erg/cm^2/s, which is entirely compatible with (8.11).

An alternative approach to the problem is as follows. We note that at the larger bubble sizes, the viscous losses from the bubble oscillation become relatively small compared to the thermal and radiation losses. Since we are close to bubble resonance, the thermal and radiation losses are comparable, so that radiation losses account for perhaps half of the energy lost from the bubble in the dominant frequency range.

Let α be the proportion of the initial energy which is converted to sound radiation. On our hypothesis $\alpha < 0.5$, say. The initial energy, in the proposed mechanism, comes entirely from initial distortions of the bubble, and is proportional to $T\Delta S$, where ΔS is the excess surface area of the bubble, beyond the equilibrium valve. If we assume that ΔS is of the same order as S, we conclude that the energy released, per unit horizontal area of the sea surface, is of order $\alpha\beta T$, where β denotes the new

† In the above calculation we have ignored the reduction in *radiation* damping due to partial cancellation of the signal by its image. This will increase the pulse length, tending to make (8.10) an underestimate.

bubble surface area created per unit time, and per unit horizontal area of the sea surface. The total sound flux F_z is then given by

$$F_z = \alpha\beta T. \tag{8.12}$$

To estimate β we have roughly

$$\beta = 4\pi a^2 b, \tag{8.13}$$

where a is a representative bubble radius and b is given by Toba's estimates. At a wind speed of 11 m/s, for instance, and with $a = 0.1$ cm, (8.2) gives $b = 0.04$. So from (8.11)

$$F_z = 2.8\alpha \text{ erg/cm}^2\text{/s}. \tag{8.14}$$

Thus everything depends upon α. There may be no better way of determining α than by a detailed calculation such as we have carried out. Nevertheless, we see that this represents at least one possible mechanism whereby surface tension energy is converted directly into acoustical energy.

9. Discussion and conclusions

An arbitrary initial distortion of a bubble will produce a monopole sound radiation, whether or not there is an initial change of volume from the equilibrium volume. Generally, volume pulsations will be excited, dominantly those close to the frequency of the 'breathing mode'. In §§2 and 3 we discussed one particular initial distortion of the bubble, of moderate amplitude. However, in the formation of closed bubbles, by whatever process, some extreme distortion is necessarily involved. At the surface of the sea, for example, pockets of air may be formed, even in light winds, by steep capillary waves (Toba 1961), or by capillary-scale features and short breaking waves. Such air pockets, initially cylindrical in form, will be unstable and will contract into spherical shapes, emitting sound in the process.

An examination of the spectral range of natural sound in the ocean, approximately 0.1 to 10^2 kHz, shows that it includes many resonances between distortion modes and the 'breaking mode'; see Paper I figure 2.

Bubble formation in the ocean will of course take place close to the surface, which is a pressure release surface. Although this tends to reduce the intensity of the radiated sound, initial bubble distortions may still contribute significantly to underwater sound in the ocean.

For information and discussions on the subject of bubbles I am particularly indebted to Dr J. Rooney and Dr R. Glazman of J.P.L., Professor M. Tulin (UC Santa Barbara), Professor A. T. Ellis (UC San Diego) and Dr F. Henyey (LJI). An excellent introduction to the subject of underwater sound came from the participants at the NATO Workshop held at Lerici, Italy, in June 1987, for which I thank especially the organizer, Dr B. Kerman.

The main results contained in this paper were presented by the author at a seminar given at MIT on 18 May 1988.

This work has been made possible by the La Jolla Institute's Independent Research and Development Fund. I am indebted to Dr R. Fitzgerald and Dr M. Orr of the Office of Naval Research for their lively interest. The work was supported under ONR Contract N00014-88C-0563.

REFERENCES

BANNER, M. H. & CATO, D. H. 1987 Physical mechanisms of noise generation by breaking waves – a laboratory study. *Proc. NATO Adv. Workshop on Natural Mechanisms of Surface Generated Noise in the Ocean, Lerici, Italy, 15–19 June 1987.* In *Sea Surface Sound* (ed. B. R. Kerman), pp. 429–436. Reidel, 639 pp.

CHANDRASEKHAR, S. 1961 *Hydrodynamic and Hydromagnetic Stability.* Clarenden. 654 pp.

DEVIN, C. 1959 Survey of thermal, radiation and viscous damping of pulsating air bubbles in water. *J. Acoust. Soc. Am.* **31**, 1654–1667.

ELLER, A. I. 1970 Damping constants of pulsating bubbles. *J. Acoust. Soc. Am.* **47**, 1469–1470.

ERDELYI, A., MAGNUS, W., OBERHETTINGER, F. & TRICOMI, F. G. 1953 *Higher Transcendental Functions*, vol. 2. McGraw-Hill. 396 pp.

FARMER, D. M. 1987 Observations of high frequency ambient sound generated by air–sea interaction processes. *Proc. NATO Adv. Workshop on Natural Mechanisms of Surface Generated Noise in the Ocean. Lerici, Italy, 15–19 June 1987.* In *Sea Surface Sound* (ed. B. R. Kerman), pp. 403–416. Reidel, 639 pp.

FARMER, D. M. & VAGLE, S. 1988 On the determination of breaking surface wave distributions using ambient sound. *J. Geophys. Res.* **93**, 3591–3600.

FITZPATRICK, H. M. & STRASBERG, M. 1957 Hydrodynamic sources of sound. *Proc. 1st Symp. on Naval Hydrodynamics, Washington, D.C.*, NAS-NRC Publ. 515, pp. 241–280. Washington, U.S. Govt. Printing Office.

HOLLETT, R. & HEITMEYER, R. 1987 Noise generation by bubbles formed in breaking waves. *Proc. NATO Adv. Workshop on Natural Mechanisms of Surface Generated Noise in the Ocean, Lerici, Italy, 15–19 June 1987.* In *Sea Surface Sound* (ed. B. R. Kerman), pp. 449–461. Reidel, 639 pp.

KIBBLEWHITE, A. C. 1987 Ocean noise spectrum below 10 Hz – mechanism and measurements. *Proc. NATO Adv. Workshop on Natural Mechanisms of Surface Generated Noise in the Ocean, Lerici, Italy, 15–19 June 1987.* In *Sea Surface Sound* (ed. B. R. Kerman), pp. 337–360. Reidel, 639 pp.

LAMB, H. 1881 On the oscillations of a viscous spheroid. *Proc. Lond. Math. Soc.* **13**, 51–66.

LAMB, H. 1932 *Hydrodynamics*, 6th edn. Cambridge University Press, 632 pp.

LONGUET-HIGGINS, M. S. 1950 A theory of the origin of microseisms. *Phil. Trans. R. Soc. Lond.* A **243**, 1–35.

LONGUET-HIGGINS, M. S. 1953 Can sea waves cause microseisms? *Proc. Symp. on Microseisms, Harriman, N.Y. Sept. 1952. NAS-NRC Publ.* **306**, pp. 74–93.

LONGUET-HIGGINS, M. S. 1983 Bubbles, breaking waves and hyperbolic jets at a free surface. *J. Fluid Mech.* **127**, 103–121.

LONGUET-HIGGINS, M. S. 1988 Limiting forms for capillary–gravity waves. *J. Fluid Mech.* **194**, 351–375.

LONGUET-HIGGINS, M. S. 1989 Monopole emission of sound by asymmetric bubble oscillations. Part 1. Normal modes. *J. Fluid Mech.* **201**, 525–541.

PROSPERETTI, A. 1977 Thermal effects and damping mechanisms in the forced radial oscillations of gas bubbles in fluids. *J. Acoust. Soc. Am.* **61**, 17–27.

TOBA, Y. 1961 Drop production by bursting of air bubbles on the sea surface (III). Study by use of a wind flume. *Mem. Coll. Sci. Univ. Kyoto* A **29**, 313–343.